All Sciences Proceedings

5th International Conference on Applied Engineering and Natural Sciences

July 10-12, 2023 : Konya, Turkey

All Sciences Proceedings
http://as-proceeding.com/

https://www.icaens.com/

Impact of Al_2O_3-Cu/Water Hybrid Nanofluid and Impinging Jet on Moving Plate at High Reynolds Numbers: A Numerical Study

Recep Ekiciler[1*]

[1*]*Mechanical Engineering, Gazi University, Ankara*

[*]*(recepekiciler@gazi.edu.tr)*

Abstract – Numerical research utilizing the commercial code ANSYS FLUENT is conducted to examine the heat transfer from a heated moving surface caused by confined slot-jet impingement at high Reynolds numbers. Confined slot-jet impingement's flow and thermal fields are studied using the SST $k-\omega$ turbulence model. Important parameters such as high Reynolds numbers (50000, 100000, and 150000), different working fluids (water and 1.0% Al_2O_3-Cu/water hybrid nanofluid), and different impinging surface velocities (V_p=0, 2, and 3 m/s) are investigated on Nusselt numbers, skin friction factors, temperature contours, and velocity streamlines. According to the results, it is determined that the Nusselt number increased as the impinging surface's velocity increased. While the Nusselt number grows with the increament in the Reynolds number, the skin friction factor tends to decrease. The utilization of 1.0% Al_2O_3-Cu/water hybrid nanofluid as the working fluid also has a substantial influence on heat transfer.

Keywords – Moving İmpinging Plate, Heat Transfer, Hybrid Nanofluid, High Reynolds Number, Skin Friction Coefficient

I. INTRODUCTION

The high heat transfer rates provided by jet impingement make it a promising cooling mechanism among the many thermal transport technologies. For this reason, many commercial processes use impinging jets, including drying paper, cooling turbine blades, cooling electronic equipment, and tempering glass [1–3].

The researchers are interested in the topic since impinging jets have practical applications and have superior benefits for future hopes in thermal management. Numerous computational and experimental studies of impinging jet heat transfer with varied working fluids and boundary conditions have been conducted in recent years. Bradbury [4] conducted experiments to examine the velocity distribution and axial velocity attenuation of a conventional single-hole free jet. According to the findings, the central region of the jet experiences high velocities, high turbulence, and very turbulent fluid mixing. Sharif and Banerjee [5] conducted an investigation of the heat tranmission resulting from the impingement of a confined slot-jet on a moving surface. The researchers analyzed the results for a range of values for the impingement plate spacing, plate normalized velocity, and jet exit Reynolds number. They found that both the plate's velocity and the jet exit Reynolds number have a significant impact on the average Nusselt number. The usage of ZnO nanofluid decreased the surface temperature of the test sample by roughly 15 percent at 180 W and heat input increased the heat flux by approximately 20.2% according to research by Khatak et al. [6]. The thermal conductivity of nanofluids including silver nanoparticles with a size range of 60-70 nm was investigated by Patel et al. [7]. The study revealed that the incorporation of silver nanoparticles at a volume fraction of 0.001% resulted in a 3% increase in the thermal conductivity of the nanofluids. Zumbrunnen [8] achieved a similar solution for a planar impinging slot-jet on a moving surface in the stagnation area. A uniform heat flux was applied to the moving surface. The findings indicated that the deceleration of boundary

layer growth caused by the motion of the plate led to an enhanced heat transfer efficiency.

In this paper, water and 1.0% Al_2O_3-Cu/water hybrid nanofluid are utilized as the working fluid for confined slot-jet impingement on heated moving plate for different high Reynolds numbers. The primary goal of the investigation is to understand the influence of the velocity of the moving plate, the Reynolds number, and the hybrid nanofluid. The flow and heat features are analyzed in detail. The outcomes of this investigation may boost the thermal efficiency of several different technology sectors.

II. Mathematical Formulation

A. Physical Description and Boundary Conditions

Figure 1 is a simplified representation of the confined impinging slot-jet with a heated moving plate that is taken into account for this research. The geometric parameters are L = 620 mm, H = 49.6 mm, and W = 6.2 mm. It is assumed that the input part of the channel has a uniform velocity, U_{in}, and temperature, T_{in} = 293 K and that the exit section of the channel has a pressure outlet condition. The no-slip flow condition is enforced on the bottom wall, which is also maintained at a constant temperature of T_w = 318 K. The top wall is no-slip flow and in adiabatic condition.

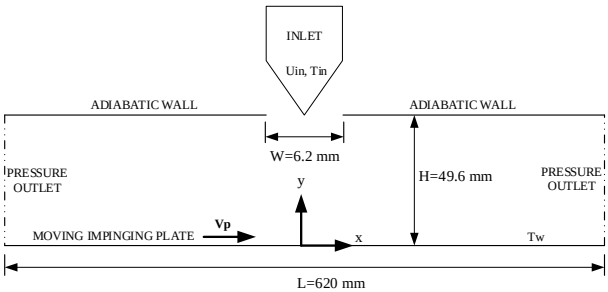

Fig. 1. Physical model of the study

B. Calculation of Hybrid Nanofluid Thermophysical Properties

In this research, the following expressions may be used to characterize the thermophysical characteristics of Al_2O_3-Cu/water hybrid nanofluid and also the thermophysical properties of Cu nanoparticles and water can be found in Ref [9] and Al_2O_3 nanoparticle properties can be found in Ref [10]:

Density [11]:

$$\rho_{hynf} = (1-\varphi)\rho_w + \varphi_{Al_2O_3}\rho_{Al_2O_3} + \varphi_{Cu}\rho_{Cu} \quad (1)$$

Specific heat [11]:

$$\left(\rho c_p\right)_{hynf} = (1-\varphi)\left(\rho c_p\right)_w + \varphi_{Al_2O_3}\left(\rho c_p\right)_{Al_2O_3} + \varphi_{Cu}\left(\rho c_p\right)_{Cu} \quad (2)$$

Thermal conductivity [12]:

$$\frac{k_{hynf}}{k_w} = -151.5\varphi^2 + 8.916\varphi + 1.004 \quad (3)$$

Viscosity [12]:

$$\frac{\mu_{hynf}}{\mu_w} = -1283\varphi^2 + 84.31\varphi + 0.9454 \quad (4)$$

C. Governing Equations

Following are the simulation's time-averaged solutions to the continuity, momentum, and energy equations:

$$\frac{\partial u_i}{\partial x_i} = 0 \quad (5)$$

$$\rho u_j \frac{\partial u_i}{\partial x_j} = -\frac{\partial P}{\partial x_i} + \frac{\partial}{\partial x_j}\left[\mu\left(\frac{\partial u_i}{\partial x_j} + \frac{\partial u_j}{\partial x_i}\right) - \rho\overline{u_i' u_j'}\right] \quad (6)$$

$$\rho u_j \frac{\partial T}{\partial x_j} = \frac{\partial}{\partial x_j}\left[\frac{\mu}{Pr}\frac{\partial T}{\partial x_j} - \rho\overline{T' u_j'}\right] \quad (7)$$

where the Reynolds stress term, denoted by the $-\rho\overline{u_i' u_j'}$, and the specific turbulent heat flux, denoted by the $\rho\overline{T' u_j'}$, are two such terms.

For k and ω, the turbulence model transport equations are [13]:

$$u_i \frac{\partial k}{\partial x_i} = \frac{\widetilde{P_k}}{\rho} - \beta^* k\omega + \frac{\partial}{\rho \partial x_i}\left[(\mu + \sigma_k \mu_T)\frac{\partial k}{\partial x_i}\right] \quad (8)$$

$$u_i \frac{\partial \omega}{\partial x_i} = \alpha S^2 - \beta \omega^2 + \frac{\partial}{\rho \partial x_i}\left[(\mu + \sigma_\omega \mu_T)\frac{\partial \omega}{\partial x_i}\right] + 2(1 - F_1)\sigma\omega_2 \frac{1}{\omega}\frac{\partial k}{\partial x_i}\frac{\partial \omega}{\partial x_i} \quad (9)$$

The turbulence model contants are:

$\beta^* = 0.09,\ \beta_1 = 3/40,\ \beta_2 = 0.0828,\ \alpha_1 = 5/9,\ \sigma_{\omega_1} = 0.5, \sigma_{k_1} = 0.85, \alpha_2 = 0.44, \sigma_{k_2} = 1, \sigma_{\omega_2} = 0.856.$

D. *Numerical Algorithm*

In order to calculate the comfined jet flow's forced convection heat transfer on the model surfaces, the Ansys Fluent 2022 R2 software is employed. The energy and momentum equations are discretized with the help of the second order upwind approach, while the turbulence equations are discretized employing the first order upwind method. The convergence criteria for all equations are set at 10^{-6} to ensure that the numerical solutions converge.

E. *Grid Optimization and Validation*

The computational domain comprised of 30998 rectangular elements. The mesh independence of the simulation is verified. In order to prove the accuracy of the study, the comparison of the skin friction coefficient and Nusselt number with a study conducted in the literature is shown in Figure 2. This study shares the same geometry as the one by Datta et al. [9] in the literature. Looking at the graph, the maximum Nusselt number and skin friction factor deviation between this study and the study in the literature are 8.78% and 11.6%, respectively.

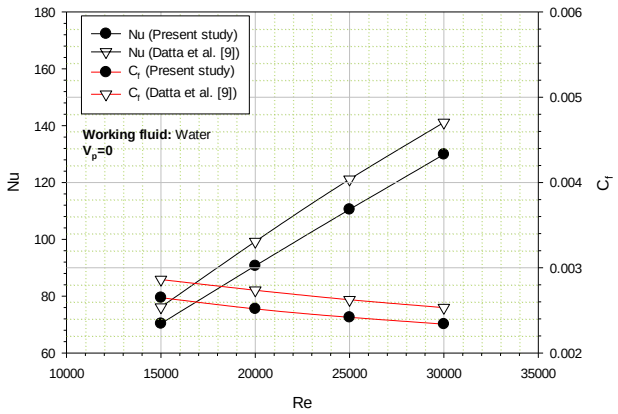

Fig. 2. Validation of the study

F. *Data Reduction*

The formula for determining the Reynolds number is as follows:

$$Re = \frac{\rho U_{in} W}{\mu} \quad (14)$$

where W and U_{in} represent the jet inlet width and velocity, respectively.

Below is a form of the equation for the Nusselt number:

$$Nu = \frac{q'' W}{k(T_w - T_{in})} \quad (15)$$

where T_w and T_{in} represent the temperature of impinging surface and inlet, respectively. q'' is the heat flux of the impinging plate.

The skin friction coefficient (C_f) equation can be stated below [14,15]:

$$C_f = \frac{2\tau_w}{\rho U_{in}^2} \quad (16)$$

where τ_w is the wall shear stress of the impinging surface.

III. Results and Discussion

Flow and heat transfer fields for different working fluids (water and 1.0% Al_2O_3-Cu/water hybrid nanofluid), impinging surface velocities (V_p=0, 2,

and 3 m/s), and high Reynolds numbers (50000-100000-150000) are shown and discussed below. In addition to the discussion, temperature contours and velocity streamlines are provided.

Figure 3 shows the Nusselt number variation at different high Reynolds numbers and the velocities of the moving plate for water and 1.0% Al_2O_3-Cu/water hybrid nanofluid, respectively. As can be seen from the graphs, the Nusselt number increases with the increase of the Reynolds number and velocity of the moving plate for both water and 1.0% Al_2O_3-Cu/water hybrid nanofluid. In addition, when 1.0% Al_2O_3-Cu/water hybrid nanofluid is used as the working fluid, the Nusselt number increases more than water.

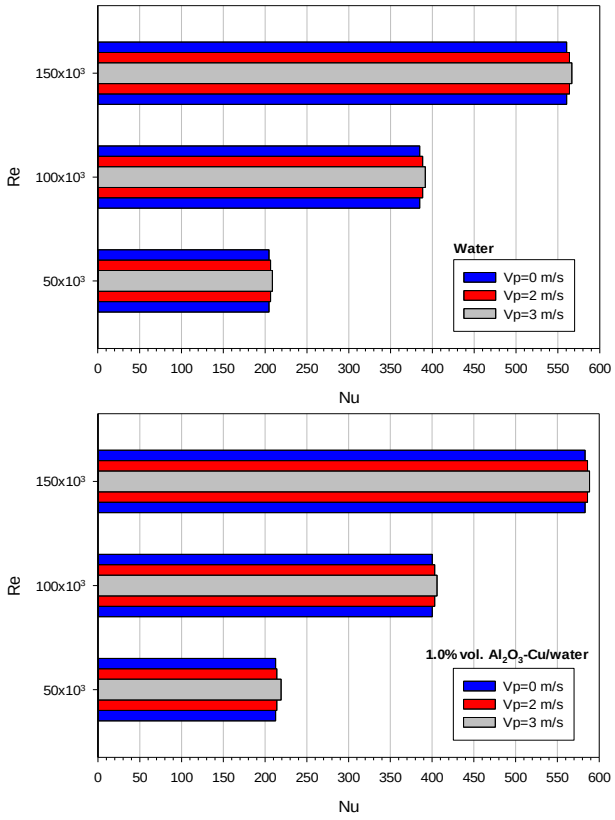

Fig. 3. Nusselt number distribution for water and 1.0% Al_2O_3-Cu/water hybrid nanofluid at various Reynolds numbers

The influences of different velocities of moving plate and Reynolds numbers on the skin friction coefficient using water and 1.0% Al_2O_3-Cu/water hybrid nanofluid are given in Figure 4. According to the graphs, regardless of the working fluid, the skin friction coefficient shows a decreasing trend due to the increase in the velocity of the working fluid depending on the increase in the Reynolds number. The skin friction coefficient rises with the use of 1.0% Al_2O_3-Cu/water hybrid nanofluid. Also, the skin friction coefficient increases in parallel with the increase in the velocity of the moving plate. The results are in agreement with Ref [16].

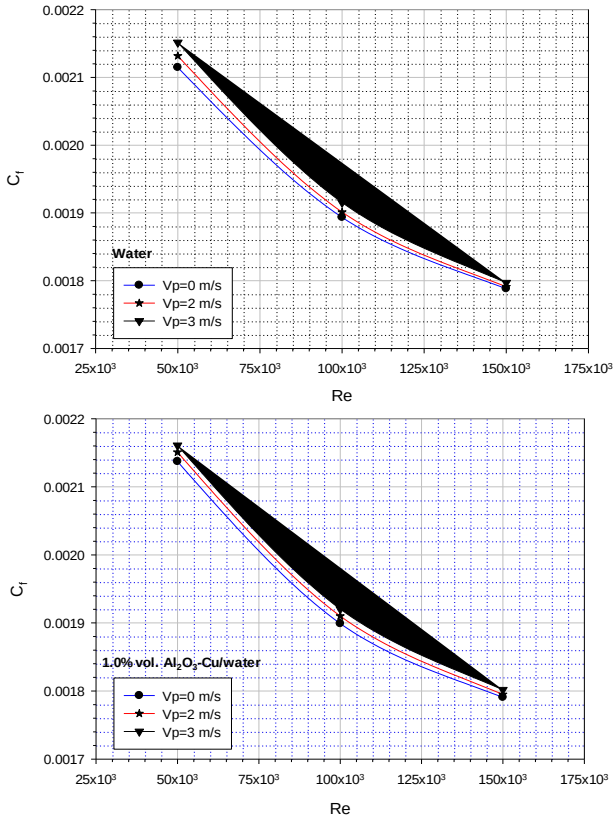

Fig. 4. Variations of skin friction coefficient at various Reynolds numbers for water and 1.0% Al_2O_3-Cu/water hybrid nanofluid

Figure 5 displays the effects of hot bottom plate velocity on the distribution of the temperature contours at Re=50000. In all working fluids, as the plate velocity increases, the thermal boundary layer thickness decreases, so an increase in heat transfer occurs. While a symmetrical temperature distribution is formed on the fixed plate, the symmetry in the temperatures is disrupted when the plate is moved.

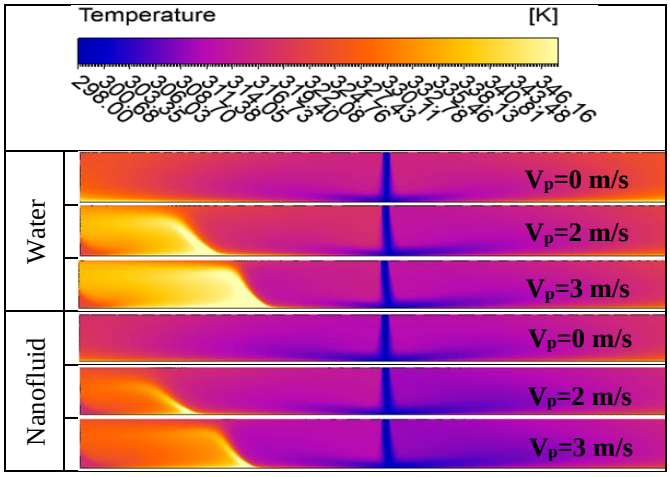

Fig. 5. Influence of the working fluids and velocity of the impinging plate on temperature contours

Velocity streamlines distributions at Re=50000 as a function of hot bottom plate's velocity for various working fluids are shown in Figure 6. When the bottom plate is at rest, the impact jet generates symmetrically a vortex on both the right and left sides of the plate for all working fluid. The velocity streamlines curve to the right when the bottom plate starts to move. An increase in the drag force acting on the fluid is responsible for this phenomenon. Streamlines of the jet stream are deflected in the moving direction due to shear stress caused by the plate's motion.

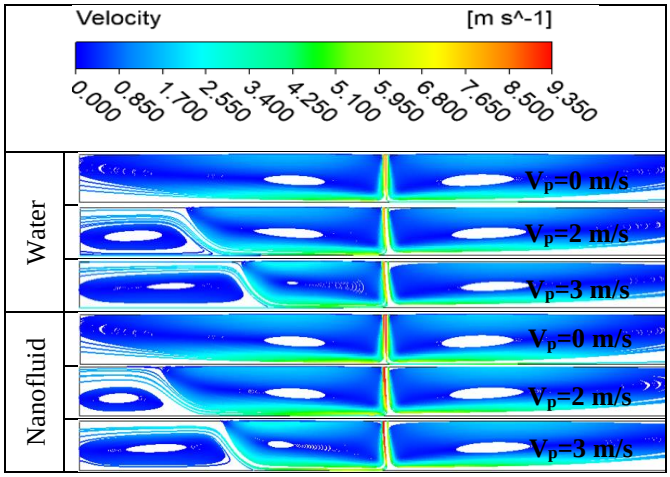

Fig. 6. Influence of the working fluids and velocity of the impinging plate on velocity streamlines

IV. CONCLUSIONS

The results of the analyses are presented as follows:

- For both water and the 1.0% Al_2O_3-Cu/water hybrid nanofluid, the Nusselt number grows in proportion to the velocity of the moving plate and the Reynolds number.
- The skin friction coefficient rises proportionally with the velocity of the moving plate.
- The uniformity of temperatures is disrupted when the plate is moved.

REFERENCES

[1] M. Amjadian, H. Safarzadeh, M. Bahiraei, S. Nazari, B. Jaberi, Heat transfer characteristics of impinging jet on a hot surface with constant heat flux using Cu_2O–water nanofluid: An experimental study, Int. Commun. Heat Mass Transf. 112 (2020) 104509.

[2] R. Kumar, R. Nadda, S. Kumar, S. Saboor, C. Ahamed Saleel, M. Abbas, A. Afzal, E. Linul, Convective heat transfer enhancement using impingement jets in channels and tubes: A comprehensive review, Alex. Eng. J. 70 (2023) 349–376.

[3] D.H. Lee, J.R. Bae, H.J. Park, J.S. Lee, P. Ligrani, Confined, milliscale unsteady laminar impinging slot jets and surface Nusselt numbers, Int. J. Heat Mass Transf. 54 (2011) 2408–2418.

[4] L.J.S. Bradbury, The structure of a self-preserving turbulent plane jet, J. Fluid Mech. 23 (1965) 31–64.

[5] M.A.R. Sharif, A. Banerjee, Numerical analysis of heat transfer due to confined slot-jet impingement on a moving plate, Appl. Therm. Eng. 29 (2009) 532–540.

[6] P. Khatak, R. Jakhar, M. Kumar, Enhancement in Cooling of Electronic Components by Nanofluids, J. Inst. Eng. India Ser. C. 96 (2015) 245–251.

[7] H.E. Patel, S.K. Das, T. Sundararajan, A. Sreekumaran Nair, B. George, T. Pradeep, Thermal conductivities of naked and monolayer protected metal nanoparticle based nanofluids: Manifestation of anomalous enhancement and chemical effects, Appl. Phys. Lett. 83 (2003) 2931–2933.

[8] D.A. Zumbrunnen, Convective Heat and Mass Transfer in the Stagnation Region of a Laminar Planar Jet Impinging on a Moving Surface, J. Heat Transf. 113 (1991) 563–570.

[9] A. Datta, S. Kumar, P. Halder, Heat Transfer and Thermal Characteristics Effects on Moving Plate Impinging

from Cu-Water Nanofluid Jet, J. Therm. Sci. 29 (2020) 182–193.

[10] W. Guo, G. Li, Y. Zheng, C. Dong, The effect of flow pulsation on Al_2O_3 nanofluids heat transfer behavior in a helical coil: A numerical analysis, Chem. Eng. Res. Des. 156 (2020) 76–85.

[11] B. Takabi, H. Shokouhmand, Effects of Al_2O_3–Cu/water hybrid nanofluid on heat transfer and flow characteristics in turbulent regime, Int. J. Mod. Phys. C. 26 (2015) 1550047.

[12] M. Mollamahdi, M. Abbaszadeh, Gh.A. Sheikhzadeh, Analytical study of Al_2O_3-Cu/water micropolar hybrid nanofluid in a porous channel with expanding/contracting walls in the presence of magnetic field, Sci. Iran. 25 (2018) 208–220.

[13] J. Issac, D. Singh, S. Kango, Experimental and numerical investigation of heat transfer characteristics of jet impingement on a flat plate, Heat Mass Transf. 56 (2020) 531–546.

[14] N.A. Kiselev, A.I. Leontiev, Yu.A. Vinogradov, A.G. Zditovets, S.S. Popovich, Heat transfer and skin-friction in a turbulent boundary layer under a non-equilibrium longitudinal adverse pressure gradient, Int. J. Heat Fluid Flow. 89 (2021) 108801.

[15] H. Coşanay, H. F. Oztop, F. Selimefendigil, A computational analysis on convective heat transfer for impinging slot nanojets onto a moving hot body, Int. J. Numer. Methods Heat Fluid Flow. 32 (2021) 364–386.

[16] B. Buonomo, O. Manca, N.S. Bondareva, M.A. Sheremet, Thermal and Fluid Dynamic Behaviors of Confined Slot Jets Impinging on an Isothermal Moving Surface with Nanofluids, Energies. 12 (2019) 2074.